Adsorption (2009) 15: 156–166
DOI 10.1007/s10450-009-9165-x

Synthesis of large-pore SBA-15 silica using poly(ethylene oxide)-poly(methyl acrylate) diblock copolymers

Liang Cao · Hongchen Dong · Liang Huang · Krzysztof Matyjaszewski · Michal Kruk

Published online: 21 March 2009

Abstract Poly(ethylene oxide)-poly(methyl acrylate) diblock copolymers with narrow molecular weight distributions were synthesized using atom transfer radical polymerization. The copolymers were used as micellar templates for the synthesis of mesoporous silicas. The products were characterized using small-angle X-ray scattering, transmission electron microscopy (TEM) and nitrogen adsorption. The obtained silicas exhibited two-dimensional hexagonal structures of cylindrical mesopores, and thus can be classified as SBA-15 silicas. In some cases, the size of ordered domains was very small. The (100) interplanar spacings were 13–17 nm, depending on the size of the diblock copolymer used and on the synthesis conditions. Nitrogen adsorption showed that the silicas exhibited specific surface areas of 350–800 $m^2\,g^{-1}$, pore volumes $\sim$1 $cm^3\,g^{-1}$, and narrow pore size distributions. The BJH (nominal) pore diameters were up to $\sim$20 nm, but actual diameters of cylindrical pores are expected to be somewhat smaller. In many cases, the mesopores exhibited constrictions.

Keywords Nitrogen adsorption · SBA-15 · Micelle-templated material · Cylindrical pore

L. Cao · L. Huang · M. Kruk (✉)
Department of Chemistry, College of Staten Island and Graduate Center, City University of New York, Staten Island, NY 10314, USA
e-mail: kruk@mail.csi.cuny.edu

H. Dong · K. Matyjaszewski
Department of Chemistry, Carnegie Mellon University, Pittsburgh, PA 15213, USA

1 Introduction

SBA-15 silica with two-dimensional (2-D) hexagonal structure of large (diameter above 5 nm) cylindrical mesopores attracted a lot of attention during the last ten years (Zhao et al. 1998a, 1998b). The interest in SBA-15 stems from several remarkable features of this material. First, the synthesis of SBA-15 is well-reproducible and based on the use of readily available poly(ethylene oxide)-poly(propylene oxide)-poly(ethylene oxide) triblock copolymers (PEO-PPO-PEO; Pluronics manufactured by BASF). It should be noted that usually the copolymers with a major fraction of the hydrophobic (PPO) block, such as Pluronic P123 ($EO_{20}PO_{70}EO_{20}$) are used as templates for SBA-15. Second, SBA-15 exhibits pore diameters larger than those attainable for well-ordered MCM-41 (up to $\sim$7 nm) and MCM-48 silicas (up to $\sim$5 nm) templated by alkylammonium surfactants (Beck et al. 1992; Kresge et al. 1992; Khushalani et al. 1995; Huo et al. 1996; Corma et al. 1997, 1998; Sayari et al. 1997b; Kruk et al. 2000b). Third, the pore diameter of SBA-15 can easily be adjusted in a wide range by changing the temperature or time of the hydrothermal treatment (Zhao et al. 1998a; Fulvio et al. 2005). Forth, SBA-15 is inherently much more hydrothermally stable than MCM-41 (Zhao et al. 1998a) and MCM-48. Fifth, the cylindrical pores of SBA-15 are usually connected with one another, due to the occlusion of the poly(ethylene oxide) blocks of the template in the silica framework (Kruk et al. 2000a; Ryoo et al. 2000), which creates opportunities for the use of SBA-15 as a template for the synthesis of ordered arrays of connected nanowires and nanotubules (Jun et al. 2000; Joo et al. 2001).

It was originally reported that the pore diameter of SBA-15 silica can be enlarged from its typical value ($\sim$9 nm) to

30 nm using Pluronic P123 ($EO_{20}PO_{70}EO_{20}$) as a surfactant template and 1,3,5-trimethylbenzene (TMB) as a swelling agent (Zhao et al. 1998a, 1998b). However, it was shown later (Lettow et al. 2000) that as the amount of TMB is increased, a limited pore diameter increase (up to 12 nm) with retention of the SBA-15 structure is followed by a major pore size increase with a change of the pore geometry to spherical and formation of a new material, referred to as a mesocellular foam (MCF) (Schmidt-Winkel et al. 1999). MCFs exhibit quite narrow pore size distributions (PSDs) and their structures are either weakly ordered or disordered.

Several strategies were reported that allow one to extend the pore diameter for SBA-15 beyond the 12 nm limit. First, the use of concentrated solutions of Pluronic F127 ($EO_{106}PO_{70}EO_{106}$) triblock copolymer (which has the same size of the hydrophobic PPO block as Pluronic P123, but has much larger hydrophilic PEO blocks), in combination with appropriate cosolvents (butanol, pentanol, hexanol), and in some cases, swelling agents (octane), afforded SBA-15 silicas with large values of (100) interplanar spacing, d_{100} (up to 17 nm) (Feng et al. 2000a, 2000b). The gas adsorption data reported for one of these materials with $d_{100} = 14.0$ nm indicated the pore diameter beyond the 12 nm limit. Recently, the use of PPO homopolymer to swell Pluronic F127 micelles afforded SBA-15 silicas with BJH pore diameters up to 13 nm (Sörensen et al. 2008). It should be noted that Pluronic F127 is usually used to template spherical rather than cylindrical pores (Zhao et al. 1998b), so the cosolvents and/or swelling agents have a strong influence on the morphology of the micellar templates. Second, the replacement of TMB with other swelling agents expanded the range of achievable pore diameters. In particular, 1,3,5-triisopropylbenzene (TIPB) was used to obtain large-pore SBA-15 (Li et al. 2002), but the quality of this material is difficult to ascertain on the basis of the limited characterization data reported. More recently, linear hydrocarbons were found suitable to tailor the pore size of SBA-15, which increased up to 15.7 nm (as estimated using BJH method) as the chain length of the alkane decreased (Sun et al. 2005; Zhang et al. 2006). The largest mesopores were synthesized using hexane as a swelling agent, which required the selection of a low initial synthesis temperature (~15 °C) (Sun et al. 2005; Zhang et al. 2006; Kruk and Cao 2007). Recently, it was found that the low-temperature synthesis using Pluronic P123 as a template and TIPB as a micelle expander afforded SBA-15 silicas with pore diameters up to 26 nm (Cao et al. 2009).

While the use of swelling agents has been an attractive strategy for the pore size enlargement since the inception of ordered mesoporous materials (Beck et al. 1992), the selection of surfactants of appropriate size is another well-established strategy for the pore size tailoring (Beck et al. 1992; Zhao et al. 1998b). Early work on the synthesis of large-pore silica with 2-D hexagonal array of cylindrical mesopores involved poly(ethylene-co-butylene)-poly(ethylene oxide) surfactants (Goltner et al. 1998), but the structural identification of the product was based only on transmission electron microscopy (TEM) and is not fully convincing. Later work involved block copolymers synthesized via the extension of PEO block with poly(methyl acrylate) (PMA) block(s) (Chan et al. 2002, 2003; Lin et al. 2006) using atom transfer radical polymerization (ATRP) (Wang and Matyjaszewski 1995; Matyjaszewski and Xia 2001). The resulting diblock (PEO-PMA) (Chan et al. 2003) and triblock (PMA-PEO-PMA) (Lin et al. 2006) copolymers were successfully used as templates for the synthesis of 2-D hexagonal silica structures (SBA-15) with d_{100} interplanar spacings up to at least 16.5 nm, and with BJH pore diameters up to 20 nm. The increase in the size of the hydrophobic block (PMA) resulted in a fairly systematic pore diameter increase. However, in the report on the use of PEO-PMA copolymers, broad ranges of synthesis conditions were delineated, with no specific conditions for the synthesis of particular samples. Moreover, only two examples of large-pore SBA-15 silicas were described in these two reports (Chan et al. 2003; Lin et al. 2006), whose adsorption isotherms were similar to those commonly observed for SBA-15 (Zhao et al. 1998a), that is, with the uptake leveling off after the capillary condensation in the primary (ordered) mesopores, and with narrow adsorption/desorption hysteresis loops with parallel branches. On the other hand, one of the reported isotherms (Chan et al. 2003) showed a hysteresis loop characteristic of a material with constricted (cage-like (Yu et al. 2000) or plugged (Van Der Voort et al. 2002; Kruk et al. 2003)) mesopores, while another one showed a significant increase in uptake extending from the capillary condensation in primary mesopores to the saturation vapor pressure. Apparently, the structures of these materials exhibited peculiarities not observed in typical SBA-15 silicas. Because of the fact that PEO-based copolymers with hydrophobic blocks other than PPO, for instance PMA or PS, can be conveniently synthesized and hold promise in the synthesis of large-pore ordered mesoporous silicas (Chan et al. 2003; Lin et al. 2006; Deng et al. 2007; Bloch et al. 2008), it is important to further investigate templating effects of these novel structure directing agents.

Herein, our work on the use of well-defined PEO-PMA diblock copolymers is reported. It is confirmed that such copolymers with high mass fraction of the PMA block are suitable as templates for large-pore SBA-15 with an appreciable degree of structural ordering. It is shown that the mesopores of these materials tend to exhibit plugs at early stages of the synthesis and the plugs can persist in the hydrothermally-treated products. The hydrothermal treatment procedure was found to have a major influence on the pore diameter of the resulting PEO-PMA-templated materials.

2 Experimental

2.1 Materials

Methyl acrylate (MA, Aldrich, 99%) was purified by filtration through a basic alumina column to remove inhibitors before the synthesis. CuBr (Aldrich, 99%) was purified via several slurries in acetic acid followed by filtration and washing with methanol and ethyl ether, and stored under nitrogen before use. Poly(ethylene oxide) (PEO) functionalized at one end with the 2-bromoisobutyrate (BiB) group was prepared via a reaction of poly(ethylene glycol) methyl ether ($M_n = 2000$ g/mol, Aldrich) with 2-bromo-2-methylpropionic acid (Aldrich, 98%), as described elsewhere (Tsarevsky et al. 2002). $CuBr_2$ (Aldrich, 99.999%), N,N,N′,N″,N″-pentamethyldiethylenetriamine (PMDETA, Aldrich, 99%), and acetone (Aldrich, >99%) were used as received.

PEO-*b*-PMA diblock copolymers were synthesized by ATRP of MA from 2-bromoisobutyrate functionalized PEO (PEO-BiB) macroinitiator. The detailed reaction conditions and results are as follows. $EO_{45}MA_{50}$ copolymer (as established using ^{1}H NMR) of molecular weight 6700 g mol^{-1} and polydispersity index of 1.07 (as measured using Gel Permeation Chromatography (GPC) in THF, based on polystyrene standards) was synthesized using acetone as a solvent at 45 °C with polymerization time of 63 hours. The initial concentration of MA was 5.5 M. The molar ratio was: PEO-BiB:MA:CuBr:$CuBr_2$:PMDETA = 1:78:0.2:0.02:0.22 (Davis et al. 2000; Matyjaszewski et al. 2000). $EO_{45}MA_{68}$ copolymer of molecular weight 8000 g mol^{-1} and polydispersity index of 1.06 was synthesized at 50 °C with polymerization time of 43 hours. The molar ratio was: PEO-BiB:MA:CuBr:$CuBr_2$:PMDETA = 1:78:0.4:0.00:0.4. In a typical reaction (synthesis of $EO_{45}MA_{50}$), PEO-BiB macroinitiator (5.0 g, 2.3 mmol), $CuBr_2$ (10.4 mg, 0.047 mmol), PMDETA (106 μL, 0.511 mmol), MA (16.4 mL, 181 mmol), and acetone (16.4 mL) were added to a 100-mL Schlenk flask equipped with a magnetic stir bar. The flask was sealed, and the resulting solution was subjected to three freeze-pump-thaw cycles. The flask was filled with nitrogen, and then while the mixture was immersed in liquid nitrogen, 66.7 mg (0.47 mmol) of CuBr was added. The flask was sealed with a glass stopper, evacuated, and back-filled with nitrogen four times. After melting the reaction mixture and warming to room temperature, the initial sample was taken and the sealed flask was placed in thermostated oil bath at 45 °C. Aliquots were removed by syringe in order to monitor molecular weight evolution. After a predetermined time, the flask was removed from the oil bath and opened to expose the catalyst to air. The polymerization solution was diluted with tetrahydrofuran (THF) and passed over an alumina (activated neutral) column to remove the catalyst. Solvent was removed by rotary evaporation, and the polymer was isolated by precipitation into methanol.

Table 1 Conditions for the synthesis of the samples

Sample	Template	Silica source	EO/Si ratio	NH_4F/Si ratio	[HCl]	T_i (°C)	T_h (°C)
68A1	$EO_{45}MA_{68}$	TEOS	0.60	0	2.0 M	10	–
68A2	$EO_{45}MA_{68}$	TEOS	0.60	0	2.0 M	10	100
68A3	$EO_{45}MA_{68}$	TEOS	0.60	0	2.0 M	10	100(W)
68B	$EO_{45}MA_{68}$	TEOS	0.75	0	2.0 M	10	100
68C	$EO_{45}MA_{68}$	TEOS	0.60	0.03	2.0 M	10	100
68D	$EO_{45}MA_{68}$	TMOS	0.60	0.03	2.0 M	10	100
68E	$EO_{45}MA_{68}$	TEOS	0.60	0.03	2.0 M	7	100
50A1	$EO_{45}MA_{50}$	TEOS	0.60	0	2.0 M	10	60
50A2	$EO_{45}MA_{50}$	TEOS	0.60	0	2.0 M	10	100
50B	$EO_{45}MA_{50}$	TEOS	0.60	0.03	0.1 M	10	100
50C	$EO_{45}MA_{50}$	TMOS	0.60	0.03	0.1 M	10	100

Notation: TEOS, tetraethyl orthosilicate; TMOS, tetramethyl orthosilicate; EO/Si ratio, molar ratio of the ethylene oxide units to silicon atoms in the silica source; NH_4F/Si, molar ratio of NH_4F to silicon atoms in the silica source; [HCl], concentration of aqueous solution of HCl used for the synthesis; T_i, initial synthesis temperature; T_h, hydrothermal treatment temperature (W denotes hydrothermal treatment of as-synthesized, filtered and dried sample in water)

The conditions of the synthesis of mesoporous silicas are summarized in Table 1. The block copolymer (∼0.50 g) was dissolved in 50 mL of an aqueous solution of HCl under stirring in a polypropylene (PP) bottle. In some cases, NH_4F (0.0053 g) was added. The solution was brought to the initial synthesis temperature (in most cases, 10 °C) using a refrigerated bath and then silica source (for instance, 0.98 g of TEOS in the synthesis of 68A1-3) was added under mechanical stirring, which continued for one day. Subsequently, the PP bottle was capped and the synthesis mixture was moved to an oven set at 100 °C (or 60 °C) and kept for one day under static conditions. In the case of sample 68A1, the product was filtered out after the initial synthesis step and a part of it was dispersed in water and heated at 100 °C for one day to obtain sample 68A3. The as-synthesized products were calcined under air at 550 °C. The samples are denoted nX, where $n = 50$ or 68 indicates the number of repeating units in the PMA block and X is a letter (A, B, C and so on) added to enumerate different synthesis conditions. If more than one sample was prepared from the same initial synthesis mixture, the letter is followed by a number 1, 2 and so on.

2.2 Measurements

Molecular weight (M_n) and polydispersity index (M_w/M_n) were determined by GPC equipped with an autosampler (Waters, 717 plus), HPLC pump with THF as eluent at 1 mL/min (Waters, 515) and four columns (guard, 10^5 Å,

10^3 Å, 100 Å; Polymer Standards Services) in series. Toluene was used as internal standard. Calculations of molar mass were determined using PSS software using a calibration based on linear polystyrene standards. The composition of the diblock copolymer or DP of PMA block was determined by ^{1}H-NMR in $CDCl_3$ on Bruker Avance 300 MHz spectrometer at 27 °C. Small-angle X-ray scattering measurements were performed at Cornell High Energy Synchrotron Source (CHESS). Nitrogen adsorption measurements at −196 °C were carried out using a Micromeritics ASAP 2020 volumetric adsorption analyzer. Prior to the adsorption measurement, the samples were outgassed under vacuum at 200 °C in the port of the gas adsorption analyzer. In some cases, low-pressure and higher-pressure data were recorded, while in most cases, low-pressure data (below the relative pressure of 0.01) were not acquired. Transmission electron microscopy (TEM) images were recorded on a Philips CM 100 microscope operated at 80 kV.

2.3 Calculations

The BET specific surface area (Sing et al. 1985) was calculated from the data in the relative pressure range of 0.04–0.2. The total pore volume (Sing et al. 1985) was evaluated from the amount adsorbed at a relative pressure of 0.99. The micropore volume, V_{mi}, was calculated using the α_s plot method (Sing et al. 1985) in the standard reduced adsorption range 0.9–1.2 (or similar). The external surface area and the sum of the primary mesopore volume, V_p, and the micropore volume, V_{mi}, were calculated using the α_s plot method in standard reduced adsorption intervals selected within the 1.8–2.3 range. In the case of some samples, the assessment of these quantities from the α_s plot analysis was not possible, as inferred from unrealistically high estimates of the external surface area. The most likely reason was that at pressures following the capillary condensation in the ordered (primary) mesopores, the multilayer adsorption on the external surface of particles was accompanied to an appreciable extent by the capillary condensation, making the considered pressure range unsuitable for surface area and pore volume calculations based on the α_s plot analysis. The reference adsorption isotherm for a macroporous silica gel was used in the α_s plot analysis (Jaroniec et al. 1999). The BJH pore size distribution was calculated from adsorption branch of the adsorption-desorption isotherm using the algorithm based on the work of Barrett, Joyner and Halenda (BJH) (Barrett et al. 1951), the Kelvin equation for the hemispherical meniscus, and the statistical film thickness curve for silicas (Jaroniec et al. 1999). Where possible, the pore diameter, w_d, was also assessed on the basis of V_{mi}, V_p, and the (100) interplanar spacing (d_{100}) calculated from SAXS data using the following relation for a honeycomb structure of cylindrical pores separated from one another with walls that exhibit additional porosity (Sayari et al. 1997a):

$$w_d = 1.213 d_{100} \left(\frac{V_p}{1/\rho + V_p + V_{mi}} \right)^{1/2} \quad (1)$$

where ρ is the silica framework density assumed to be 2.2 g cm^{-3}.

3 Results and discussion

It was first attempted to carry out the synthesis of ordered mesoporous silicas using $EO_{45}MA_{68}$ block copolymer template at room temperature or slightly above it (~30 °C), which is in the temperature range employed earlier in the mesoporous silica synthesis with similar copolymer templates (Chan et al. 2003). However, the products exhibited moderate structural ordering and some undesirable features, such as onion-shaped structures, as seen from TEM. The onion-shaped structures may be vesicles (Yu et al. 2001) or curved 2-D hexagonally ordered bundles of cylindrical pores (Sun et al. 2006). As the synthesis temperature was lowered, the structural ordering improved and temperature of 10 °C was selected in most of our synthesis work. Shown in Fig. 1 are SAXS patterns for samples synthesized at an initial temperature of 10 °C, either without subsequent hydrothermal treatment (68A1), or with the treatment at 100 °C for one day, in either the original synthesis mixture (68A2), or water (68A3). The peaks on the patterns can be indexed as reflections of the 2-D hexagonal structure. In particular, five peaks were observed on the pattern for sample 68B2. The (100)

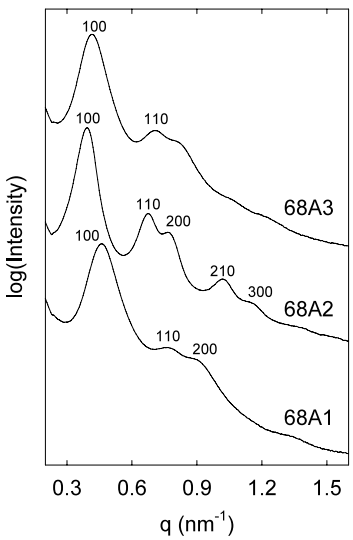

Fig. 1 SAXS patterns for calcined silicas templated by $EO_{45}MA_{68}$ and synthesized without the hydrothermal treatment (68A1), with hydrothermal treatment in the synthesis mixture (68A2) and with hydrothermal treatment in water (68A3)

Table 2 The structural parameters of the samples assessed from small-angle X-ray scattering data

Sample	$d_{100,uc}$ (nm)	d_{100} (nm)	$d_{100}/d_{100,uc}$
68A1	–	13.7	–
68A2	17.0	16.0	0.94
68A3	–	14.8	–
68B	16.9	16.2	0.96
68C	16.8	16.3	0.97
68D	17.1	16.7	0.97
68E	17.0	16.2	0.96
50A1	15.1	13.1	0.87
50A2	15.1	14.3	0.95
50B	14.7	13.8	0.94
50C	14.8	14.3	0.97

Notation: $d_{100,uc}$, (100) interplanar spacing for uncalcined sample; d_{100}, (100) interplanar spacing for calcined sample; $d_{100}/d_{100,uc}$, ratio of interplanar spacings after and before calcination

interplanar spacings, d_{100}, determined from SAXS data are listed in Table 2. It should be noted that d_{100} multiplied by 1.155 provides the unit-cell parameter, a, which is equal to the distance between the centers of adjacent pores in the honeycomb structure. The unit cell parameter is a sum of the pore diameter and the pore wall thickness (in the thinnest point).

The calcined sample obtained with the hydrothermal treatment of the synthesis mixture at 100 °C exhibited the highest (100) interplanar spacing (16.0 nm) among the considered samples. This value was 6% lower than the interplanar spacing for as-synthesized (uncalcined) material, showing that the shrinkage upon calcination was moderate. The (100) interplanar spacing of 16.0 nm is comparable to those attained for SBA-15 templated by $MA_{70}EO_{77}MA_{70}$ triblock copolymer (Lin et al. 2006) and by $EO_{127}PO_{70}EO_{127}$ using alcohols as cosolvents (Feng et al. 2000a), while it is larger than the interplanar spacings for SBA-15 synthesized using $EO_{20}PO_{70}EO_{20}$ as a template and alkanes as micelle expanders (Zhang et al. 2006). On the other hand, TIPB in combination with $EO_{20}PO_{70}EO_{20}$ template affords even larger unit-cell sizes (d_{100} up to 26 nm) (Cao et al. 2009).

As expected from the work on large-pore SBA-15 templated by Pluronics (Kruk and Cao 2007), and the study of porous silicas templated by poly(ethylene oxide)-polyacrylonitrile (PEO-PAN) copolymers (Kruk et al. 2006), the calcined sample synthesized without the hydrothermal treatment exhibited much smaller interplanar spacing. An unexpected finding was that the hydrothermal treatment in water, which was employed in earlier studies of silicas templated by PEO-PMA copolymers (Chan et al. 2003; Lin et al. 2006), afforded a unit-cell size significantly smaller than

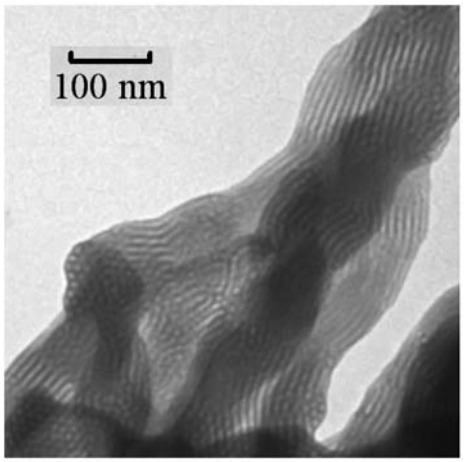

Fig. 2 TEM image of calcined silica templated by $EO_{45}MA_{68}$ and synthesized by employing hydrothermal treatment of the synthesis mixture (68A2)

that attained after the hydrothermal treatment in the synthesis mixture. Also, in the former case, the SAXS pattern was less resolved. Therefore, in the reminder of this paper, the discussion will be focused on silicas whose synthesis involved the hydrothermal treatment of the synthesis mixture.

The 2-D hexagonal ordering of sample 68A2 was additionally confirmed by TEM, which showed honeycomb patterns and series of parallel stripes (see Fig. 2). Interestingly enough, the lateral size of ordered domains was small (∼10–15 repeating units). Also, defects in the 2-D hexagonal arrangement related to merging (or splitting) of adjacent mesopores were clearly visible (see upper part of Fig. 2).

Nitrogen adsorption isotherms for the samples from 68A series are shown in Fig. 3. The sample 68A1 synthesized without the hydrothermal treatment had an isotherm with a very broad adsorption-desorption hysteresis loop that closed at the lower limit of adsorption-desorption hysteresis (relative pressure 0.40–0.50) (Kruk and Jaroniec 2003). Similar hysteresis loops were reported earlier for SBA-15 silica templated by $EO_{45}MA_{72}$ copolymer and hydrothermally treated in water (Chan et al. 2003), and for SBA-15 synthesized at low temperature without subsequent hydrothermal treatment, using hexane as a swelling agent (Kruk and Cao 2007). This behavior can be attributed to the occurrence of constrictions (plugs) in the mesopores of SBA-15 (Van Der Voort et al. 2002; Kruk et al. 2003). It appears that the micelle cores composed of hydrophobic blocks (PMA) of the template molecules solubilize the silica precursor (TEOS or products of its partial hydrolysis). The sample 68A2 obtained after the hydrothermal treatment of the synthesis mixture exhibited a hysteresis loop with a prominent tail, suggesting that the treatment reduced, but not fully eliminated the constrictions. The sample obtained after the hydrothermal treatment in water (68A3) exhibited an intermediate hysteresis loop shape, suggesting that the treatment in wa-

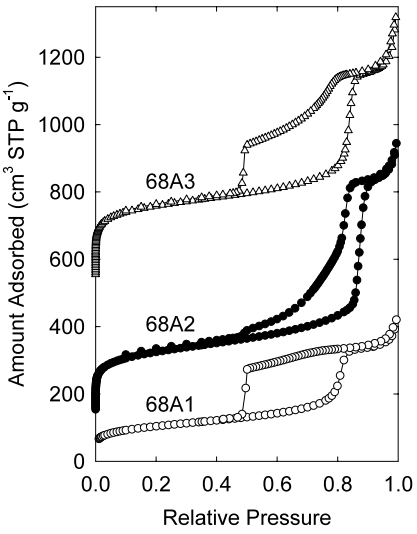

Fig. 3 Nitrogen adsorption isotherms for calcined silicas templated by $EO_{45}MA_{68}$ and synthesized without the hydrothermal treatment (68A1), with hydrothermal treatment in the synthesis mixture (68A2) and with hydrothermal treatment in water (68A3). For clarity, the isotherms for samples 68A2 and 68A3 were offset vertically by 150 and 550 cm^3 STP g^{-1}, respectively

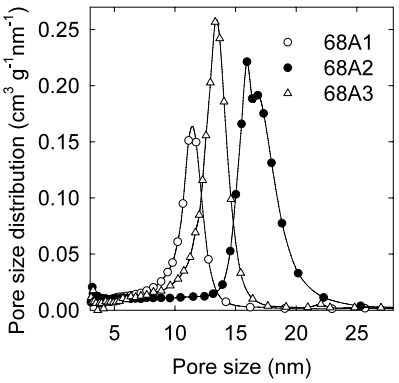

Fig. 4 Pore size distributions for calcined silicas templated by $EO_{45}MA_{68}$ and synthesized without the hydrothermal treatment (68A1), with hydrothermal treatment in the synthesis mixture (68A2) and with hydrothermal treatment in water (68A3)

ter was not as effective in eliminating the constrictions as the direct heating of the synthesis mixture was.

As seen in Fig. 4, the hydrothermal treatments resulted in the pore diameter enlargement, which was more significant in the case of the treatment in the synthesis mixture. On the other hand, the treatment in water led to a narrower pore size distribution (PSD). This behavior followed the trend observed for silicas templated by PEO-PAN block copolymers (Kruk et al. 2006). In addition to the increase in the pore diameter, the hydrothermal treatments increased the specific surface area, the total pore volume, the mesopore volume as well as the micropore volume (Table 3). For the considered samples, it was possible to use the α_s plot analysis for data

Table 3 The structural parameters of the samples determined from gas adsorption data

Sample	S_{BET} ($m^2\ g^{-1}$)	V_t ($cm^3\ g^{-1}$)	V_{mi} ($cm^3\ g^{-1}$)	V_p ($cm^3\ g^{-1}$)	S_{ext} ($m^2\ g^{-1}$)	w_{BJH} (nm)	w_d (nm)
68A1	369	0.61	0.06	0.37	94	11.4	10.8
68A2	620	1.17	0.12	0.73	192	16.3	14.5
68A3	734	1.13	0.19	0.56	187	13.3	12.2
68B	633	1.35	0.12	NA	NA	19.8	ND
68C	578	1.49	0.09	NA	NA	19.9	ND
68D	568	1.45	0.08	NA	NA	20.9	ND
68E	564	1.31	0.10	NA	NA	19.3	ND
50A1	647	0.74	0.18	0.50	37	11.2	10.5
50A2	614	0.95	0.16	0.71	45	13.3	12.6
50B	722	1.08	0.13	0.74	121	12.6	12.5
50C	802	1.16	0.19	0.72	127	12.6	12.6

Notation: S_{BET}, BET specific surface area; V_t, total pore volume; V_{mi}, micropore volume; V_p, primary mesopore volume; S_{ext}, external surface area; w_{BJH}, pore diameter estimated using the BJH method; w_d, pore diameter evaluated using (1). NA not possible to assess with acceptable accuracy using the α_s plot method. ND not determined due to the lack of estimate of V_p

at pressures above the completion of the capillary condensation step, so the primary mesopore volume was estimated and used to get an estimate of the actual pore size based on (1) (see Table 3). One finds that sample 68A2 exhibited the pore diameter of 14.5 nm, which is fairly large. It is notable that the BJH method appears to overestimate the pore diameter by 0.5–2 nm for these samples and the magnitude of the overestimation increases as the pore diameter raises above 10 nm. This is consistent with our earlier work on large-pore SBA-15 synthesized using Pluronic P123 and hexane (Kruk and Cao 2007).

As discussed above, our initial synthesis procedure afforded mesopores with constrictions. Several strategies were employed in order to eliminate these constrictions. First, TEOS/$EO_{45}MA_{68}$ ratio was reduced, because in the case of SBA-15, constrictions (plugs) in the mesopores can form for high silica-precursor/surfactant ratio (Kruk et al. 2003). This reduction of the amount of TEOS led to silica 68B with somewhat less well-resolved SAXS pattern, which was characteristic of 2-D hexagonal structure (Fig. 5). TEM confirmed the 2-D hexagonal ordering, but revealed a small ordered domain size (see Fig. 6). Nitrogen adsorption isotherm (Fig. 7) featured a narrow hysteresis loop with nearly no tailing, thus showing that the constrictions were eliminated. However, PSD broadened and showed some signs of bimodality, as the main peak appeared to be preceded by a smaller peak, which was not fully separated from the main peak. The cause of the bimodality is not clear. SAXS showed only one series of peaks for 2-D hexagonal structure, thus suggesting that only one phase was present. It was suspected

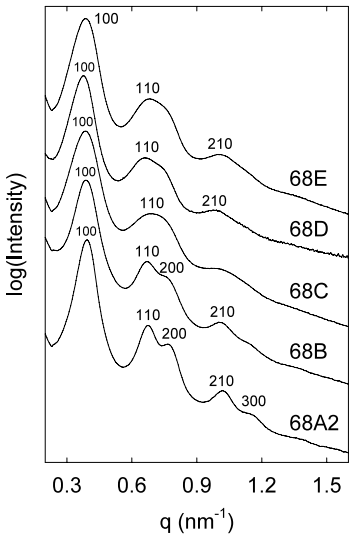

Fig. 5 SAXS patterns for calcined silicas synthesized under different conditions using $EO_{45}MA_{68}$ as a template

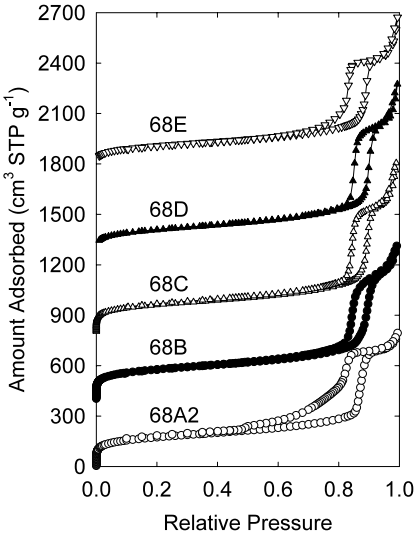

Fig. 7 Nitrogen adsorption isotherm for calcined silicas synthesized under different conditions using $EO_{45}MA_{68}$ as a template. For clarity, the isotherms for samples 68B, 68C, 68D and 68E were offset vertically by 400, 800, 1250 and 1750 cm^3 STP g^{-1}, respectively

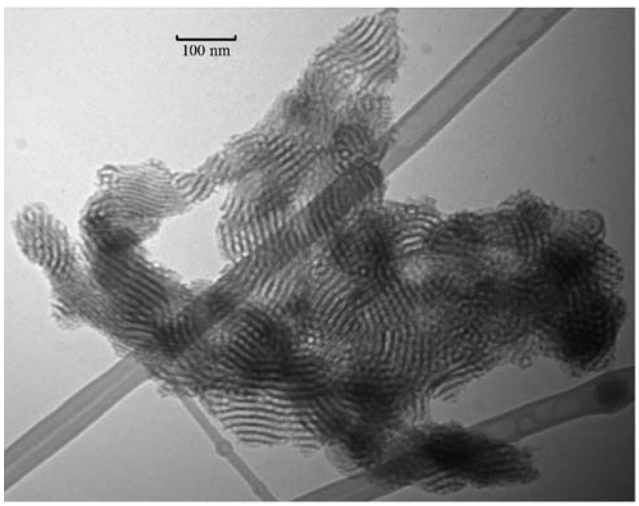

Fig. 6 TEM image of calcined silica 68B templated by $EO_{45}MA_{68}$ and synthesized with a decreased amount of TEOS (higher EO/Si ratio)

that perhaps low silica-precursor/surfactant ratio may lead to the formation of defects in the pore wall structure, which may be responsible for the bimodality. The second approach to eliminate the constrictions was based on the hypothesis that the constrictions arise from the solubilization of the silica source in the hydrophobic cores of the micelles. It was expected that the introduction of NH_4F, which facilitates the hydrolysis and condensation of silica, may lead to the presence of less hydrophobic silica species in the synthesis mixture and thus to the decrease in tendency to the solubilization of silica species in the cores of the micelles. This in turn would reduce the occurrence of constrictions in the mesopores. As seen in Fig. 5, the resulting samples 68C, 68D and 68E exhibited broader SAXS patterns in comparison to samples discussed earlier. Anyway, these patterns could still be attributed to the 2-D hexagonal structure. PSDs of these samples were narrower than those for sample 68B which had a better resolved SAXS pattern, so the broadening of the SAXS patterns for the considered samples may originate from further decrease in the ordered domain size (see Fig. 9 for the TEM image of sample 68E) rather than from the loss of correlation between the position of adjacent mesopores. Among the samples synthesized with addition of NH_4F, it is noteworthy that the replacement of TEOS (used in case of sample 68C) with faster-hydrolyzing TMOS (sample 68D) afforded a material with somewhat better resolved SAXS pattern. The decrease in the initial synthesis temperature from 10 to 7 °C (sample 68E) led not only to a better resolved SAXS pattern (compare with 68C), but to a narrower PSD (see Fig. 8). On the other hand, the tailing on the desorption branch of the hysteresis loop was more prominent for sample 68E. TEM for sample 68E (Fig. 9) showed very uniform cylindrical mesopores arranged in very small ordered domains. Some of these domains resembled bundles of tubes.

The $EO_{45}MA_{68}$-templated silicas with no appreciable constrictions in the pore structure (68B-68E) had appreciably higher BJH pore diameters when compared to the sample 68A2, which exhibited plugged mesopores, despite the fact that the (100) interplanar spacings were similar for all these samples (see Tables 2 and 3). The origin of this behavior is not fully clear. One is tempted to conclude that the presence of constrictions lowers the capillary condensation pressure in a manner resembling classical consideration of capillary condensation in open cylinders vs. adsorption

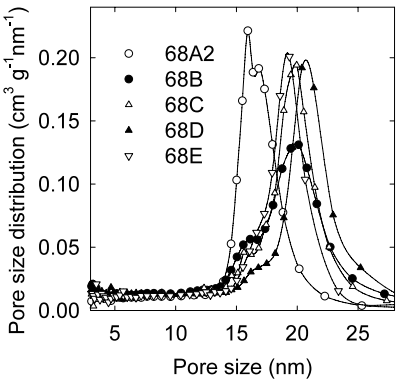

Fig. 8 Pore size distributions for calcined silicas synthesized under different conditions using $EO_{45}MA_{68}$ as a template

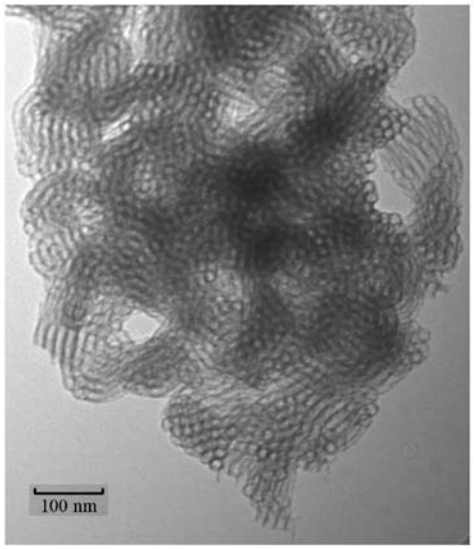

Fig. 9 TEM image of calcined silica 68E templated by $EO_{45}MA_{68}$ and synthesized a lower initial temperature (7 °C) in the presence of NH_4F

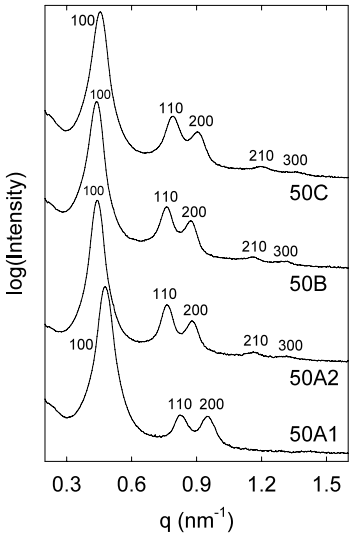

Fig. 10 SAXS patterns for calcined silicas synthesized under different conditions using $EO_{45}MA_{50}$ as a template

in pores closed at one end (Gregg and Sing 1982). However, this is rather unlikely, because the capillary condensation pressure for sample 68A2 was related to the pore diameter (calculated using (1)) in a way similar to that observed for large-pore SBA-15 silicas with no constrictions in the mesopores (Cao et al. 2009; Kruk and Cao 2007). It is more likely that the small length of the pores in materials 68B-E (as seen for sample 68B and 68E from TEM) led to the capillary condensation at somewhat higher pressure when compared with longer cylindrical pores (Stroud et al. 2001), which results in larger pore diameter assessed from the capillary condensation pressure using the BJH method. The pore wall structure of the considered samples may also feature large gaps, similarly to those in SBA-15 synthesized under specific conditions (Fan et al. 2001), resulting in some extent of pore merging and thus increasing the capillary condensation pressure beyond the point for isolated cylindrical mesopores of given size.

As discussed above, the silicas templated with $EO_{45}MA_{68}$ block copolymer exhibited 2-D hexagonal ordering, but they formed ordered domains of quite small size and their SAXS patters were not particularly well resolved. The $EO_{45}MA_{68}$ copolymer has a fairly long hydrophobic block and it may take more than ten hours to obtain its homogeneous solution in 2 M HCl. On the basis of our earlier study of silicas templated by PEO-PAN copolymers, which tend to be poorly soluble in water (Kruk et al. 2006), it was expected that the solubility issues may limit the quality of the templated silicas. Therefore, the opportunity of the synthesis of large-pore SBA-15 using $EO_{45}MA_{50}$ copolymer with a shorter hydrophobic block was also explored. As can be seen in Fig. 10, the samples exhibited SAXS patterns characteristic of 2-D hexagonal structure. (110) and (200) peaks were well resolved, unlike in cases of the silicas templated by the block copolymer with a longer hydrophobic block. The SAXS patterns for samples 50A2, 50B and 50C, whose preparation involved the heating of the synthesis mixture at 100 °C, showed (210) and (300) peaks, thus resembling the patterns of well-ordered large-pore SBA-15 synthesized using Pluronic P123 as a template and hexane as a swelling agent (Zhang et al. 2006; Kruk and Cao 2007). The considered materials also had a similar d_{100} of ~14 nm. It is noteworthy that sample 50A1 synthesized with hydrothermal treatment at 60 °C exhibited somewhat smaller interplanar spacing due to larger shrinkage upon calcination.

Nitrogen adsorption isotherms of SBA-15 silicas templated by $EO_{45}MA_{50}$ copolymer are shown in Fig. 11 and the structural parameters derived from them are listed in

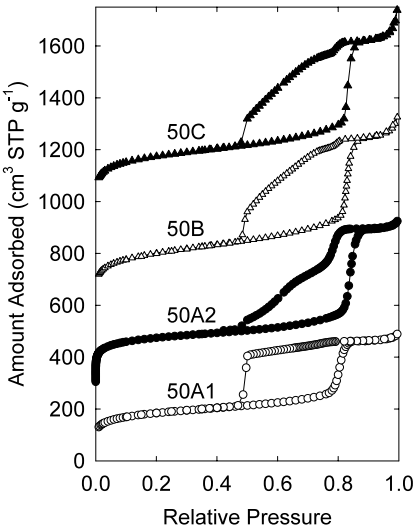

Fig. 11 Nitrogen adsorption isotherms for calcined silicas synthesized under different conditions using $EO_{45}MA_{50}$ as a template. For clarity, the isotherms for samples 50A2, 50B, and 50C were offset vertically by 300, 600 and 950 cm^3 STP g^{-1}, respectively

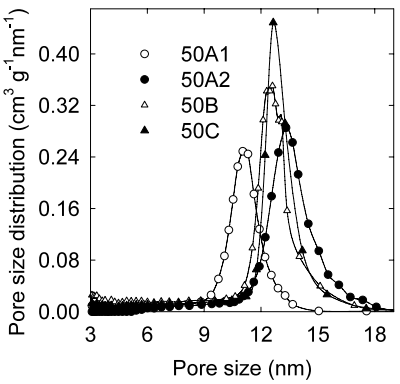

Fig. 12 Pore size distributions for calcined silicas synthesized under different conditions using $EO_{45}MA_{50}$ as a template

Table 3. The samples exhibited sharp capillary condensation steps and had quite large pore diameters (see Fig. 12 and Table 3), although the latter were lower than those of silicas synthesized with the larger $EO_{45}MA_{68}$ copolymer under the same conditions (compare 68A2 with 50A2). The latter observation confirms that ability to tailor the pore diameter by adjusting the size of the hydrophobic block in PEO-PMA copolymers (Chan et al. 2003). Interestingly enough, the samples templated by the smaller copolymer ($EO_{45}MA_{50}$) exhibited a more pronounced broadening of the hysteresis loops than their counterparts synthesized using the larger copolymer ($EO_{45}MA_{68}$). Notably, the sample 50A1 hydrothermally treated at 60 °C exhibited an isotherm with desorption primarily at the lower limit of adsorption-desorption hysteresis. This indicates that the formation of the constrictions (plugs) was more extensive when the copolymer template with shorter hydrophobic block was used. On the basis of this observation, it becomes more clear why the adsorption isotherm for SBA-15 silica templated by $EO_{45}MA_{72}$ reported by others (Chan et al. 2003) exhibited a very broad hysteresis loop, while a material templated by $EO_{45}MA_{94}$ with a larger hydrophobic block exhibited an isotherm with a narrow hysteresis loop.

In the case of both considered copolymer templates, washed and filtered as-synthesized silica/copolymer composites obtained after the hydrothermal treatment at 100 °C for one day exhibited a rather low copolymer content, as seen from thermogravimetry. Also, it was verified in several cases that the extension of the hydrothermal treatment time from one day to two days did not result in any appreciable pore diameter increase, unlike in the case of silicas templated by Pluronic copolymers. It was suspected that the copolymer may gradually decompose in 2 M HCl during the prolonged heating at 100 °C. To decrease a likelihood of such an event, the concentration of the acid was decreased to 0.1 M. This slowed down the silica hydrolysis and condensation, so NH_4F was necessary to observe the precipitation within 24 hours of the low-temperature step of the synthesis. This synthesis approach allowed us to obtain SBA-15 samples with very narrow PSD, especially in the case where TMOS was used as a silica source (sample 50C). However, the resulting materials exhibited prominent constrictions in the mesopores, as seen from the shape of the adsorption-desorption hysteresis loop.

As seen in Table 3, the PEO-PMA-templated silicas with 2-D hexagonal structures exhibited specific surface areas of 550–800 $m^2\ g^{-1}$. The total pore volume was on the order of 1 $cm^3\ g^{-1}$, and the micropore volume was on the order of 0.1 $cm^3\ g^{-1}$.

In the work with PMA-PEO-PMA copolymers as templates for SBA-15, propanol was added to the aqueous solution of HCl (Lin et al. 2006), but its role was not explained. In our low-temperature synthesis with $EO_{45}MA_{68}$ template, the addition of propanol allowed us to obtain a sample with better resolved SAXS pattern and with narrow hysteresis loop, indicating the lack of constrictions in mesopores, but the pore diameter was smaller and PSD was broader. Perhaps the addition of propanol hinders the solubilization of TEOS in hydrophobic blocks of the micellar templates.

4 Conclusions

The current study confirmed that poly(ethylene oxide)-poly(methyl acrylate) diblock copolymers are suitable as templates for the synthesis of large-pore SBA-15 silicas. Our study showed that low temperatures (e.g., 10 °C) afford materials with improved ordering. The obtained SBA-15 silicas exhibited (100) interplanar spacings up to 17 nm and often

had narrow pore size distributions. The unit-cell size and the pore diameter increased and the degree of structural ordering decreased with the increase in size of the hydrophobic block (PMA) of the copolymer. The pore size can be additionally adjusted by changing the conditions of the hydrothermal treatment. For silicas templated with the larger copolymer ($EO_{45}MA_{68}$), TEM confirmed the presence of ordered cylindrical mesopores, but showed that the lateral sizes of ordered domains were small. Nitrogen adsorption revealed that the cylindrical mesopores featured constrictions, which in many cases can be eliminated by adjusting the synthesis conditions, although this is accompanied by the lowering of the degree of structural ordering.

Acknowledgements M.K. acknowledges partial support from the Dean of Science and Engineering, CSI/CUNY and from the Center for Engineered Polymeric Materials funded by the New York State Office of Science, Technology and Academic Research (NYSTAR). SAXS measurements were performed at the Cornell High Energy Synchrotron Source (CHESS, Cornell University), which is supported by the National Science Foundation under award DMR-0225180. Dr. Detlef M. Smilgies (CHESS, Cornell University) is gratefully acknowledged for assistance in the SAXS measurements. Mr. Manik Mandal (CSI) is acknowledged for help with TEM imaging.

References

Barrett, E.P., Joyner, L.G., Halenda, P.P.: The determination of pore volume and area distributions in porous substances. I. Computations from nitrogen isotherms. J. Am. Chem. Soc. **73**, 373–380 (1951)

Beck, J.S., Vartuli, J.C., Roth, W.J., Leonowicz, M.E., Kresge, C.T., Schmitt, K.D., Chu, C.T.W., Olson, D.H., Sheppard, E.W., McCullen, S.B., Higgins, J.B., Schlenker, J.L.: A new family of mesoporous molecular sieves prepared with liquid crystal templates. J. Am. Chem. Soc. **114**, 10834–10843 (1992)

Bloch, E., Phan, T., Bertin, D., Llewellyn, P., Hornebecq, V.: Direct synthesis of mesoporous silica presenting large and tunable pores using BAB triblock copolymers: Influence of each copolymer block on the porous structure. Microporous Mesoporous Mater. **112**, 612–620 (2008)

Cao, L., Man, T., Kruk, M.: Synthesis of ultra-large-pore SBA-15 silica with two-dimensional hexagonal structure using triisopropylbenzene as micelle expander. Chem. Mater. **21**, 1144–1153 (2009)

Chan, Y.-T., Lin, H.-P., Mou, C.-Y., Liu, S.-T.: Ia3d Cubic mesoporous silicas using EO17MA23 diblock copolymers made from ATRP. Chem. Commun. 2878–2879 (2002)

Chan, Y.T., Lin, H.P., Mou, C.Y., Liu, S.T.: Synthesis of mesoporous silicas with different pore-size by using EO(m)MA(n) diblock copolymers of tunable block length as the templates. Stud. Surf. Sci. Catal. **146**, 113–116 (2003)

Corma, A., Kan, Q., Navarro, M.T., Perez-Pariente, J., Rey, F.: Synthesis of MCM-41 with different pore diameters without addition of auxiliary organics. Chem. Mater. **9**, 2123–2126 (1997)

Corma, A., Kan, Q., Rey, F.: Synthesis of Si and Ti-Si-MCM-48 mesoporous materials with controlled pore sizes in the absence of polar organic additives and alkali metal ions. Chem. Commun. 579–580 (1998)

Davis, K.A., Charleux, B., Matyjaszewski, K.: Preparation of block copolymers of polystyrene and poly(t-butyl acrylate) of various molecular weights and architectures by atom transfer radical polymerization. J. Polym. Sci., Part A: Polym. Chem. **38**, 2274–2283 (2000)

Deng, Y., Yu, T., Wan, Y., Shi, S., Meng, Y., Gu, D., Zhang, L., Huang, Y., Liu, C., Wu, X., Zhao, D.: Ordered mesoporous silicas and carbons with large accessible pores templated from amphiphilic diblock copolymer poly(ethylene oxide)-b-polystyrene. J. Am. Chem. Soc. **129**, 1690–1697 (2007)

Fan, J., Yu, C., Wang, L., Tu, B., Zhao, D., Sakamoto, Y., Terasaki, O.: Mesotunnels on the silica wall of ordered SBA-15 to generate three-dimensional large-pore mesoporous networks. J. Am. Chem. Soc. **123**, 12113–12114 (2001)

Feng, P., Bu, X., Pine, D.J.: Control of pore sizes in mesoporous silica templated by liquid crystals in block copolymer-cosurfactant-water systems. Langmuir **16**, 5304–5310 (2000a)

Feng, P., Bu, X., Stucky, G.D., Pine, D.J.: Monolithic mesoporous silica templated by microemulsion liquid crystals. J. Am. Chem. Soc. **122**, 994–995 (2000b)

Fulvio, P.F., Pikus, S., Jaroniec, M.: Tailoring properties of SBA-15 materials by controlling conditions of hydrothermal synthesis. J. Mater. Chem. **15**, 5049–5053 (2005)

Goltner, C.G., Berton, B., Kramer, E., Antonietti, M.: Nanoporous silica from amphiphilic block copolymer (ABC) aggregates: control over correlation and architecture of cylindrical pores. Chem. Commun. 2287–2288 (1998)

Gregg, S.J., Sing, K.S.W.: Adsorption, Surface Area and Porosity. Academic Press, London (1982)

Huo, Q., Margolese, D.I., Stucky, G.D.: Surfactant control of phases in the synthesis of mesoporous silica-based materials. Chem. Mater. **8**, 1147–1160 (1996)

Jaroniec, M., Kruk, M., Olivier, J.P.: Standard nitrogen adsorption data for characterization of nanoporous silicas. Langmuir **15**, 5410–5413 (1999)

Joo, S.H., Choi, S.J., Oh, I., Kwak, J., Liu, Z., Terasaki, O., Ryoo, R.: Ordered nanoporous arrays of carbon supporting high dispersions of platinum nanoparticles. Nature **412**, 169–172 (2001)

Jun, S., Joo, S.H., Ryoo, R., Kruk, M., Jaroniec, M., Liu, Z., Ohsuna, T., Terasaki, O.: Synthesis of new, nanoporous carbon with hexagonally ordered mesostructure. J. Am. Chem. Soc. **122**, 10712–10713 (2000)

Khushalani, D., Kupermann, A., Ozin, A., Tanaka, K., Garces, J., Olken, M.M., Neil, C.: Metamorphic materials. Restructuring siliceous mesoporous materials. Adv. Mater. **7**, 842–846 (1995)

Kresge, C.T., Leonowicz, M.E., Roth, W.J., Vartuli, J.C., Beck, J.S.: Ordered mesoporous molecular sieves synthesized by a liquid-crystal template mechanism. Nature **359**, 710–712 (1992)

Kruk, M., Cao, L.: Pore size tailoring in large-pore SBA-15 silica synthesized in the presence of hexane. Langmuir **23**, 7247–7254 (2007)

Kruk, M., Jaroniec, M.: Argon adsorption at 77 K as a useful tool for the elucidation of pore connectivity in ordered materials with large cagelike mesopores. Chem. Mater. **15**, 2942–2949 (2003)

Kruk, M., Jaroniec, M., Ko, C.H., Ryoo, R.: Characterization of the porous structure of SBA-15. Chem. Mater. **12**, 1961–1968 (2000a)

Kruk, M., Jaroniec, M., Ryoo, R., Joo, S.H.: Characterization of MCM-48 silicas with tailored pore sizes synthesized via a highly efficient procedure. Chem. Mater. **12**, 1414–1421 (2000b)

Kruk, M., Jaroniec, M., Joo, S.H., Ryoo, R.: Characterization of regular and plugged SBA-15 silicas by using adsorption and inverse carbon replication and explanation of the plug formation mechanism. J. Phys. Chem. B **107**, 2205–2213 (2003)

Kruk, M., Dufour, B., Celer, E.B., Kowalewski, T., Jaroniec, M., Matyjaszewski, K.: Well-defined polyethylene oxide-polyacrylonitrile diblock copolymers as templates for mesoporous silicas and precursors for mesoporous carbons. Chem. Mater. **18**, 1417–1424 (2006)

Lettow, J.S., Han, Y.J., Schmidt-Winkel, P., Yang, P., Zhao, D., Stucky, G.D., Ying, J.Y.: Hexagonal to mesocellular foam phase transition in polymer-templated mesoporous silicas. Langmuir **16**, 8291–8295 (2000)

Li, B., Inagaki, S., Miyazaki, C., Takahashi, H.: Synthesis of highly ordered large size mesoporous silica and effect of stabilization as enzyme supports in organic solvent. Chem. Res. Chinese Univ. **18**, 200–205 (2002)

Lin, C.-F., Lin, H.-P., Mou, C.-Y., Liu, S.-T.: Periodic mesoporous silicas via templating of new triblock amphiphilic copolymers. Microporous Mesoporous Mater. **91**, 151–155 (2006)

Matyjaszewski, K., Xia, J.: Atom transfer radical polymerization. Chem. Rev. **101**, 2921–2990 (2001)

Matyjaszewski, K., Shipp, D.A., McMurtry, G.P., Gaynor, S.G., Pakula, T.: Simple and effective one-pot synthesis of (meth)acrylic block copolymers through atom transfer radical polymerization. J. Polym. Sci. Part A: Polym. Chem. **38**, 2023–2031 (2000)

Ryoo, R., Ko, C.H., Kruk, M., Antochshuk, V., Jaroniec, M.: Block-copolymer-templated ordered mesoporous silica: array of uniform mesopores or mesopore-micropore network? J. Phys. Chem. B **104**, 11465–11471 (2000)

Sayari, A., Kruk, M., Jaroniec, M.: Characterization of microporous-mesoporous MCM-41 silicates prepared in the presence of octyltrimethylammonium bromide. Catal. Lett. **49**, 147–153 (1997a)

Sayari, A., Liu, P., Kruk, M., Jaroniec, M.: Characterization of large-pore MCM-41 molecular sieves obtained via hydrothermal restructuring. Chem. Mater. **9**, 2499–2506 (1997b)

Schmidt-Winkel, P., Lukens, W.W. Jr., Zhao, D., Yang, P., Chmelka, B.F., Stucky, G.D.: Mesocellular siliceous foams with uniformly sized cells and windows. J. Am. Chem. Soc. **121**, 254–255 (1999)

Sing, K.S.W., Everett, D.H., Haul, R.A.W., Moscou, L., Pierotti, R.A., Rouquerol, J., Siemieniewska, T.: Reporting physisorption data for gas/solid systems with special reference to the determination of surface area and porosity (Recommendations 1984). Pure Appl. Chem. **57**, 603–619 (1985)

Sörensen, M.H., Corkery, R.W., Pedersen, J.S., Rosenholm, J., Alberius, P.C.: Expansion of the F127-templated mesostructure in aerosol-generated particles by using polypropylene glycol as a swelling agent. Microporous Mesoporous Mater. **113**, 1–13 (2008)

Stroud, W.J., Curry, J.E., Cushman, J.H.: Capillary condensation and snap-off in nanoscale contacts. Langmuir **17**, 688–698 (2001)

Sun, J., Zhang, H., Ma, D., Chen, Y., Bao, X., Klein-Hoffmann, A., Pfaender, N., Su, D.S.: Alkanes-assisted low temperature formation of highly ordered SBA-15 with large cylindrical mesopores. Chem. Commun. 5343–5345 (2005)

Sun, J., Ma, D., Zhang, H., Bao, X., Weinberg, G., Su, D.: Macro-mesoporous silicas complex and the carbon replica. Microporous Mesoporous Mater. **100**, 356–360 (2006)

Tsarevsky, N.V., Sarbu, T., Goebelt, B., Matyjaszewski, K.: Synthesis of styrene-acrylonitrile copolymers and related block copolymers by atom transfer radical polymerization. Macromolecules **35**, 6142–6148 (2002)

Van Der Voort, P., Ravikovitch, P.I., De Jong, K.P., Benjelloun, M., Van Bavel, E., Janssen, A.H., Neimark, A.V., Weckhuysen, B.M., Vansant, E.F.: A new templated ordered structure with combined micro- and mesopores and internal silica nanocapsules. J. Phys. Chem. B **106**, 5873–5877 (2002)

Wang, J.-S., Matyjaszewski, K.: Controlled/"living" radical polymerization. Atom transfer radical polymerization in the presence of transition-metal complexes. J. Am. Chem. Soc. **117**, 5614–5615 (1995)

Yu, C., Yu, Y., Zhao, D.: Highly ordered large caged cubic mesoporous silica structures templated by triblock PEO-PBO-PEO copolymer. Chem. Commun. 575–576 (2000)

Yu, K., Hurd, A.J., Eisenberg, A., Brinker, C.J.: Syntheses of silica/polystyrene-block-poly(ethylene oxide) films with regular and reverse mesostructures of large characteristic length scales by solvent evaporation-induced self-assembly. Langmuir **17**, 7961–7965 (2001)

Zhang, H., Sun, J., Ma, D., Weinberg, G., Su, D.S., Bao, X.: Engineered complex emulsion system: toward modulating the pore length and morphological architecture of mesoporous silicas. J. Phys. Chem. B **110**, 25908–25915 (2006)

Zhao, D., Feng, J., Huo, Q., Melosh, N., Frederickson, G.H., Chmelka, B.F., Stucky, G.D.: Triblock copolymer syntheses of mesoporous silica with periodic 50 to 300 angstrom pores. Science **279**, 548–552 (1998a)

Zhao, D., Huo, Q., Feng, J., Chmelka, B.F., Stucky, G.D.: Nonionic triblock and star diblock copolymer and oligomeric surfactant syntheses of highly ordered, hydrothermally stable, mesoporous silica structures. J. Am. Chem. Soc. **120**, 6024–6036 (1998b)